Canadian Mineralogist
Vol. 31, pp. 105-117 (1993)

TEM STUDY OF INDIUM- AND COPPER-BEARING GROWTH-BANDED SPHALERITE

RICHARD A.D. PATTRICK, MARIA DORLING AND DAVID A. POLYA
Department of Geology, The University of Manchester, Manchester M13 9PL, England

ABSTRACT

An investigation by transmission electron microscopy of (Cu, In)-rich bands in sphalerite from base-metal veins in West Shropshire, England, revealed these elements to be preferentially substituted near the inner margins of the (Fe,Cd)-rich layers within the zoned grains. The iron-rich bands, furthermore, comprise several iron-rich and iron-poor sub-bands, the former containing oriented rows of "chalcopyritic" particles, probably formed by exsolution. Opaque zones of sphalerite developed adjacent to late chalcopyrite are enriched in copper but contain no microscopic particles. High-resolution microscopy of the opaque sphalerite reveals the presence of Guinier–Preston (GP) zones representing the early development of chalcopyrite. Equilibrium precipitation in response to changes in solution chlorinity, temperature and $f(O_2)$ cannot satisfactorily explain the observed banding. Instead, the repetitive chemical separation of (Cu,In)- and (Fe,Cd)-rich bands is ascribed to the preferential irreversible adsorption of these ions over differing ranges of pH during cyclic changes of solution pH. The pattern of banding caused by such a mechanism is consistent with that expected from a consideration of the first hydrolysis constants of the trace element cations.

Keywords: transmission electron microscopy, sphalerite, indium, banding, hydrolysis, adsorption, cyclicity, West Shropshire, England.

SOMMAIRE

Nous avons utilisé la microscopie électronique par transmission afin de caractériser les couches riches en cuivre et indium de la sphalérite provenant de fissures minéralisées du district de West Shropshire, en Angleterre. Ces éléments semblent incorporés préférentiellement près de la bordure interne de couches riches en Fe et Cd. De plus, les couches riches en fer sont faites de plusieurs sous-couches enrichies ou appauvries en fer. Celles qui sont les plus riches contiennent, en rangées orientées, des particules "chalcopyritiques" qui résulteraient d'une exsolution. Les zones opaques qui se sont développées dans la sphalérite tout près de la chalcopyrite tardive font preuve d'un enrichissement en Cu, mais ne contiennent pas de particules fines. Une étude des zones opaques par microscopie à haute résolution démontre le développement de zones de Guinier–Preston, qui représentent un développement précoce de la chalcopyrite. Une précipitation à l'équilibre en fonction de changements en chlorinité de la solution, en température et en $f(O_2)$ n'explique pas la zonation en couches successives. Nous croyons plutôt que la séparation répétée de Cu+In et Fe+Cd en couches est le résultat d'une adsorption irréversible préférentielle de ces ions à des valeurs de pH différentes au cours de changements cycliques du pH de la solution. L'agencement cyclique des couches qu'a causé un tel phénomène concorde avec ce que nous attendons à partir des constantes de la première hydrolyse des ions de ces métaux.

(Traduit par la Rédaction)

Mots-clés: microscopie électronique par transmission, sphalérite, indium, zonation en couches, hydrolyse, adsorption, cyclicité, West Shropshire, Angleterre.

INTRODUCTION

Trace amounts of indium commonly have been detected in sphalerite, the main source for the metal. The nature of the substitution of the indium is, however, not well understood. Incorporation as In_2S_3 was suggested by Anderson (1953), but the very low solubilities of indium in ZnS as observed in experimental studies led Kissin (1972) to suggest the presence of submicroscopic particles of an indium-bearing phase. Similarly, experimental studies have demonstrated the low solubility of Cu in sphalerite at low temperatures (Wiggins & Craig 1980). Results of electron-microprobe analysis reveal a correlation between the In and Cu content in ZnS, indicating either the coupled substitution of Cu + In or the inclusion of roquesite, $CuInS_2$ (Johan 1988, Burke & Kieft 1980, Hak *et al.* 1983). Substitution would be in the form $Cu^+ + In^{3+} \rightarrow 2Zn^{2+}$ and is facilitated by the structural similarity between roquesite and sphalerite. Indium in sphalerite also has been observed to concentrate in specific zones within the chemically variable growth-bands commonly developed in hydrothermal sphalerite (Johan 1988, Oen *et al.* 1980).

In this study, banded crystals of indium-bearing sphalerite from a base-metal vein deposit are investigated by analytical electron microscopy (AEM) with the aim of determining the nature of indium and copper substitution and examining the causes of their concentration. The indium and copper are associated with (Fe + Cd)-rich bands in the sphalerite. Possible equilibrium and kinetic mechanisms for the origin of this chemical zoning are discussed.

MINERALOGY

The samples come from an example of unmetamorphosed base-metal vein-type mineralization hosted by Ordovician greywackes in the West Shropshire Orefield, England. Galena, sphalerite and minor, paragenetically late, chalcopyrite are present and are associated with barite, calcite, witherite and, very rarely, fluorite (Pattrick & Bowell 1991). Three chemically and texturally distinct generations of sphalerite have been recognized. An optical study showed the second generation of sphalerite to be color-banded; analysis of samples from four localities revealed a sphalerite stratigraphy of the type recorded by Barton *et al.* (1977) and McLimans *et al.* (1980) throughout the orefield. The color-banded growth zones are typically pale (yellow) bands 100–200 μm wide separated by sharply defined dark (brown) bands, usually 10–100 μm in width (Fig. 1). Some of these dark bands comprise several dark and light sub-bands (~ 3–10 μm across) parallel or at a very low angle to the margins of the main bands. Associated with the darker sub-bands are lines of tiny particles. These particles are either parallel to the sub-bands or form parallel arrays at a low angle (<5°) to the sub-band margins, giving the impression of cross-stratification (Fig. 2). Adjacent to late chalcopyrite-bearing veins, the sphalerite commonly is opaque, although no inclusions were observed in it.

FIG. 1. Photomicrograph of banded sphalerite showing iron-rich bands, which appear black.

SPHALERITE CHEMISTRY

There is a relationship between color and chemistry, as demonstrated by electron-microprobe analysis (EMPA), with the darker bands containing higher concentrations of Fe (up to 6.0 wt%) and Cd (0.89 wt%) than the pale bands (Fe ≈ 2.7 wt% and Cd ≈ 0.28 wt%) (Table 1). EMPA also revealed zones enriched in both In and Cu coincident with the dark Fe-rich bands. These zones are typically less than 8 μm across, occurring either within or at the margins of the dark bands. Where associated with thicker dark bands, they occur at or close to the inner (earliest formed) margin of the band.

The results (Table 1, Fig. 3) reveal a clear positive correlation between Fe and Cd, and between Cu and In, but no direct correlation between the In and Fe contents (Fig. 3). In the indium-rich zones, the indium values rise from below detection limits (200 ppm) up to 2.4 wt%, although values of 0.4–1.0 wt% are more typical. Background values of Cu in the sphalerite are ~ 0.05 wt% but increase to 0.5 wt% in the indium-rich zones; the highest levels of copper coincide with the highest levels of indium (Fig. 3). At low concentrations of In and Cu (~ 0.3 atomic %), the ratio between these elements is 1:1, but at higher concentrations of both elements, the proportion of indium exceeds that of Cu, commonly by more than 2:1.

Although the indium-rich zones show lateral variations in concentration over a few millimeters, they are

TABLE 1. REPRESENTATIVE COMPOSITIONS* OF SPHALERITE

Zn	Fe	Cd	In	Cu	S	Total	
61.35	2.93	0.89	2.46	0.41	32.64	100.68	In-rich band
59.90	4.43	0.59	0.66	0.18	33.34	99.10	In-rich band
61.85	2.81	0.26	2.75	0.48	32.56	100.71	In-rich band
61.28	4.06	0.32	1.51	0.32	33.15	100.64	In-rich zone
64.67	3.07	0.17	0.00	0.05	33.05	101.01	Pale band
62.86	5.49	0.89	0.02	0.06	32.34	101.66	Dark band

*Electron-microprobe data, compositions given in wt%.

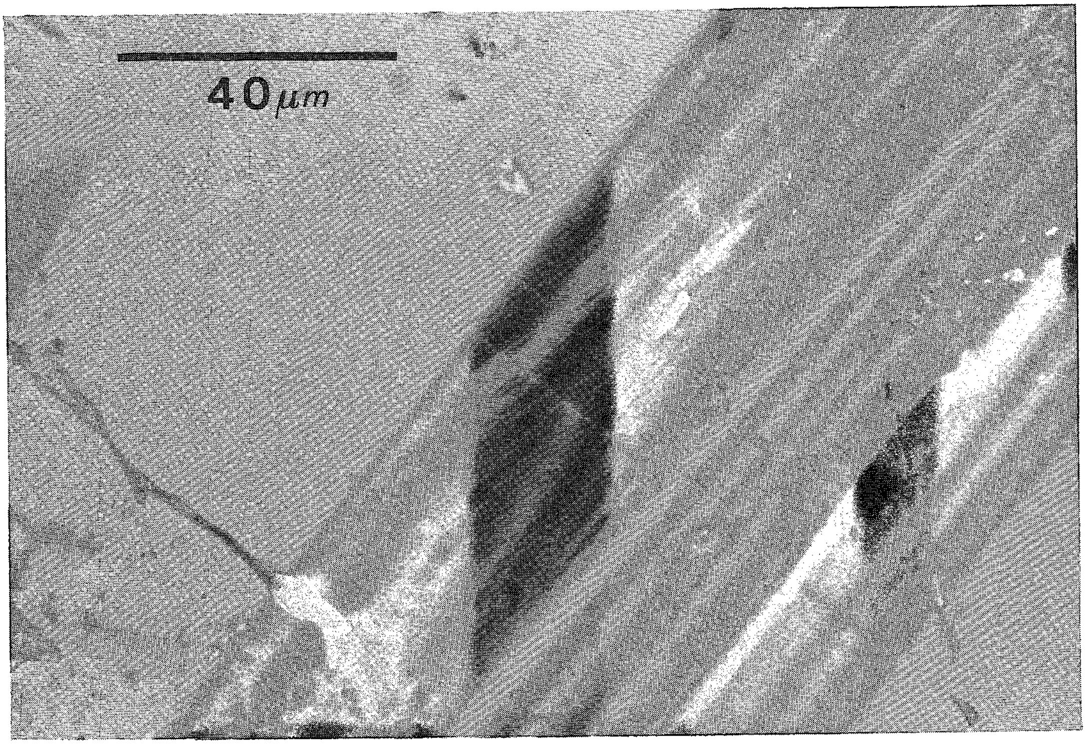

FIG. 2. Photomicrograph of an iron-rich band showing the microstructure of the band. The darker areas contain high concentrations of tiny particles.

nonetheless identifiable in sphalerite from the different mines in the area and are particularly useful in defining the band stratigraphy, effectively forming indium-rich marker horizons.

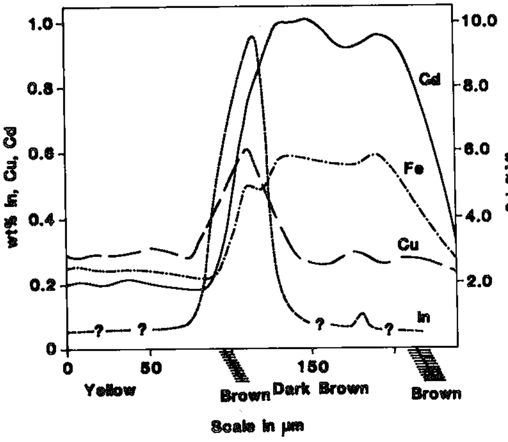

FIG. 3. Results of electron-probe microanalyses across an iron-rich band, showing the distribution of Fe, Cd, In and Cu (after Pattrick & Bowell 1991).

ELECTRON MICROSCOPY

Samples that had been subjected to investigation by optical microscopy and EMPA were prepared for a study using transmission electron microscopy (TEM) by ion-beam thinning using the technique described by Tighe (1976). The study employed a Philips EM430T instrument operating at 300 kV. Analysis was carried out using an EDAX energy-dispersion system using the correction procedures for thickness decribed by Cliff & Lorimer (1975). By photographing the samples before EMPA and after thinning, the exact position of the areas of interest could be located. The darker (iron-rich) bands are easy to identify because their higher content of Fe (2–4 wt%) made these much more resistant to thinning than the iron-poor bands.

The indium-rich zones

The inner boundary of the Fe-rich bands is sharp, with a rise in Fe occurring over a distance less than 200 Å. EDAX analysis of the bands produced results similar to those derived by EMPA. Several indium-rich zones identified by EMPA were investigated by TEM, including bands in which the Cu:In ratio is 1:1 and bands with indium in excess over copper. Although the EDAX system has higher limits of detection (for indium and copper, ~ 0.4 wt%) and lower precision than the electron microprobe, it was possible to locate the high-indium zones. These are 1–3 μm in width and usually associated with lower contents of iron within the high-iron bands. In the six bands investigated, *no* particles were observed in the indium-rich zones, either In-rich particles, such as roquesite, or Cu-rich particles. At magnifications of up to 50,000 times, the sphalerite seems clear and structureless. High-resolution microscopy (500,000 ×) revealed the sphalerite to have a perfect lattice, although some dislocations were observed.

The band microstructure and chemistry

The TEM investigation was carried out on the Fe-rich bands to determine the nature of the microstructure (sub-bands) seen in thin section. The iron-poor bands, bands with a low relative level of iron (<4 wt% Fe) and thin Fe-rich bands proved to be largely featureless. Dislocations and twinning were only rarely seen, although twin-related domains are locally intense, especially in the Fe-rich bands. Fractures also were observed; these may be decorated by euhedral inclusions (<1 μm) of calcite. Diffraction analysis revealed crystallographic continuity across the bands.

In concordance with the optical observations, the wider iron-rich bands were found to be inhomogeneous. At lower magnifications (2100 ×), the clearly defined dark and lighter "sub-bands" were revealed, caused by differential ion-beam thinning. In addition, thinning accentuated 120° grain boundaries formed during recrystallization of the sphalerite. A set of parallel, late, deformation-induced twins also are present, these corresponding to a cross-cutting linear feature observed in thin section (Fig. 4). At higher magnifications, a high

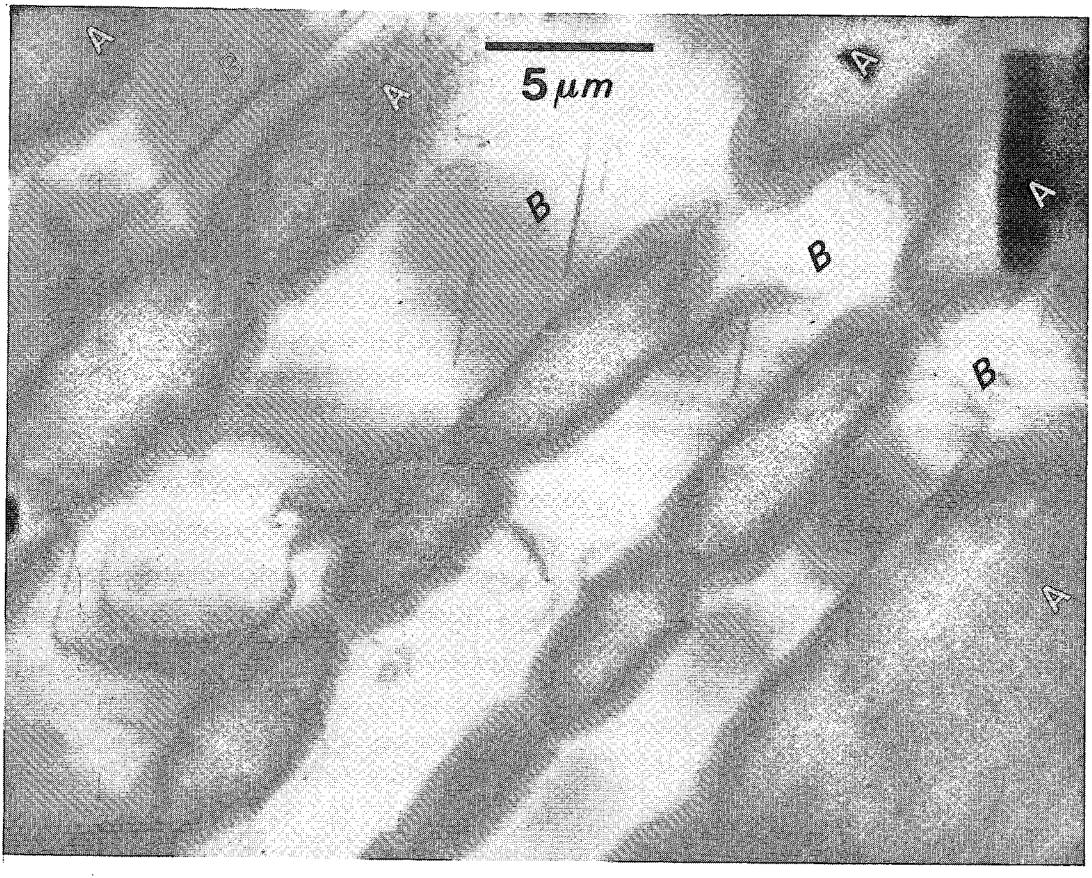

FIG. 4. Electron micrograph of an iron-rich band in sphalerite revealing alternating particle-rich (A) and particle-free (B) sub-bands. The particles are probably chalcopyrite and have developed in relatively iron-rich sub-bands. The 120° grain boundaries due to recrystalization of the sphalerite and late deformation twins are evident (see text).

density of particulate inclusions become clearly visible in the darker sub-bands. The inclusions are aligned in rows parallel to the sub-band margins (Fig. 4). Single rows of inclusions may be present within the bands, whereas thicker sub-bands may contain many rows of such particles. EDAX analyses reveal that the darker sub-bands contain approximately 0.6 wt% more iron than the lighter bands, which explains the differential thinning.

In a 200-μm-wide Fe-rich band, a well-developed repetitive sequence of particle-rich and particle-poor sub-bands is developed. This sequence comprises (in the direction of growth) 2-μm-wide sub-bands with an increasing number of particles that abruptly terminate, followed by a 0.7-μm-wide particle-free band (Fig. 5). Analysis of the sphalerite revealed variations in the iron content, with the base of the particle-free zone containing 3.2 wt% Fe, increasing to 3.6 wt% in the middle of the clear zone, and 4.8 wt% just before the particle-rich zone. The matrix in the particle-rich area contains ~ 5.0 wt% Fe, and this drops abruptly to 3 wt% again in the next particle-free zone. Cadmium also displays a positive correlation with the iron, but the concentration of copper is too close to its detection limit for the method to provide meaningful data.

Analysis of the particles proved difficult because of their small size. Even in nanoprobe mode, the volume of the particle is too small (<5% of the analyzed volume).

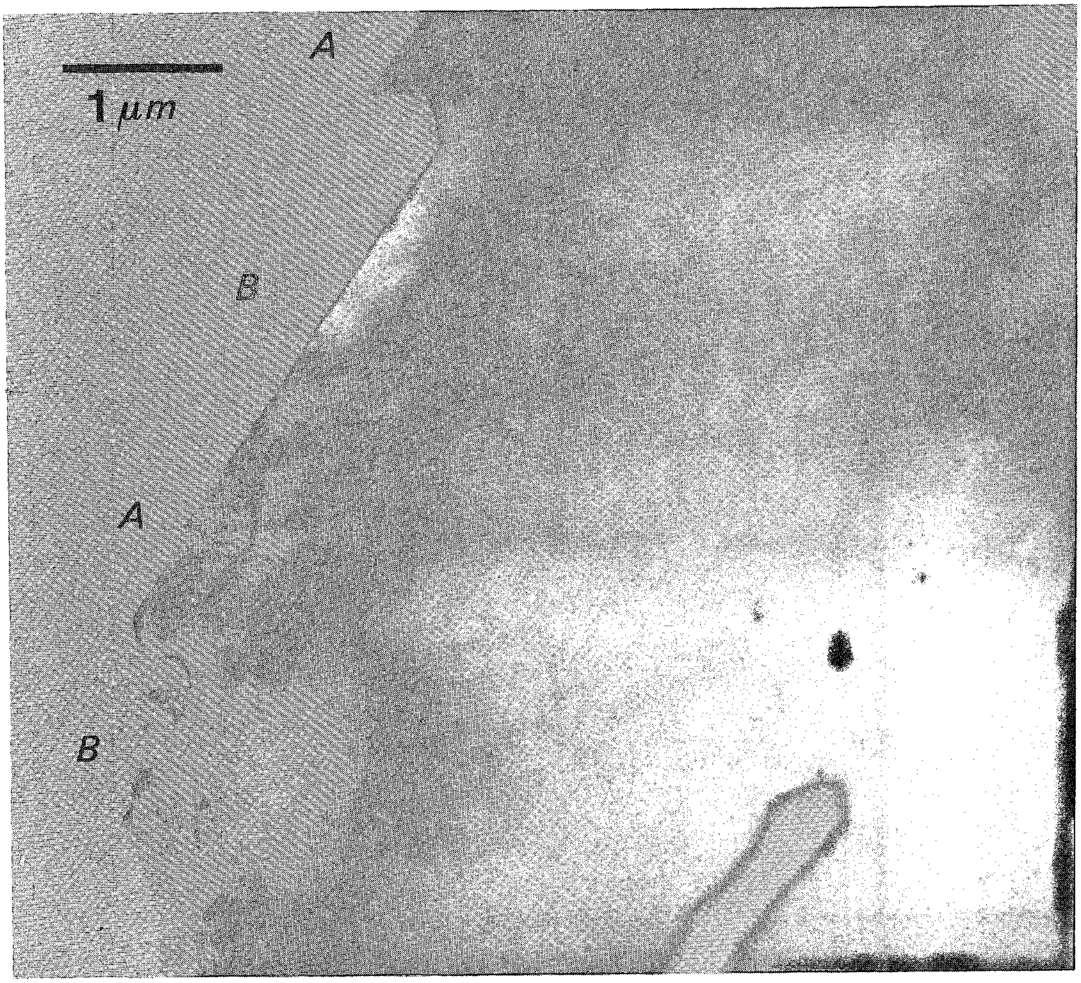

FIG. 5. Electron micrograph of part of a well-developed repetitive sequence of particle-rich (B) and particle-free sphalerite (A). The direction of crystal growth was from bottom to top.

However, by comparing results of analysis of the particles and the adjacent matrix, it was possible to demonstrate an enrichment of Cu and Fe in the particles in a 1:1 ratio, suggesting them to be either Cu+Fe sulfide (chalcopyrite) or, much less likely, Cu+Fe+Zn sulfides.

Opaque sphalerite

EMPA analysis of the opaque zones demonstrated an enrichment in Cu of up to 1.5 wt%. The presence of chalcopyrite in the cross-cutting veins suggests that these zones might contain a dusting of chalcopyrite particles formed by replacement of the iron-bearing sphalerite (chalcopyrite disease, see Barton & Bethke 1987). TEM observations showed that particles are absent; however, the sphalerite was found to be intensely twinned, with voids developed at the twin intersections (Fig. 6). This development of twins may well be related to the fracturing of the sphalerite during the formation of the cross-cutting vein. Examination of twinned areas using high-resolution microscopy (500,000 ×) did, however, reveal zones of twinning developed in the sphalerite in two directions parallel to {111} (Figs. 7, 8). These features have all the characteristics of Guinier–Preston (GP) zones, as described in silicate minerals by Champness & Lorimer (1976) and Nord (1980), which represent the first stage of phase separation in the process of exsolution. A diffraction pattern (SAED) from this area (Fig. 9) shows intense streaking between positions of the matrix reflections. This corresponds to the presence of very thin platelets in the sphalerite matrix, such as is seen in GP zones.

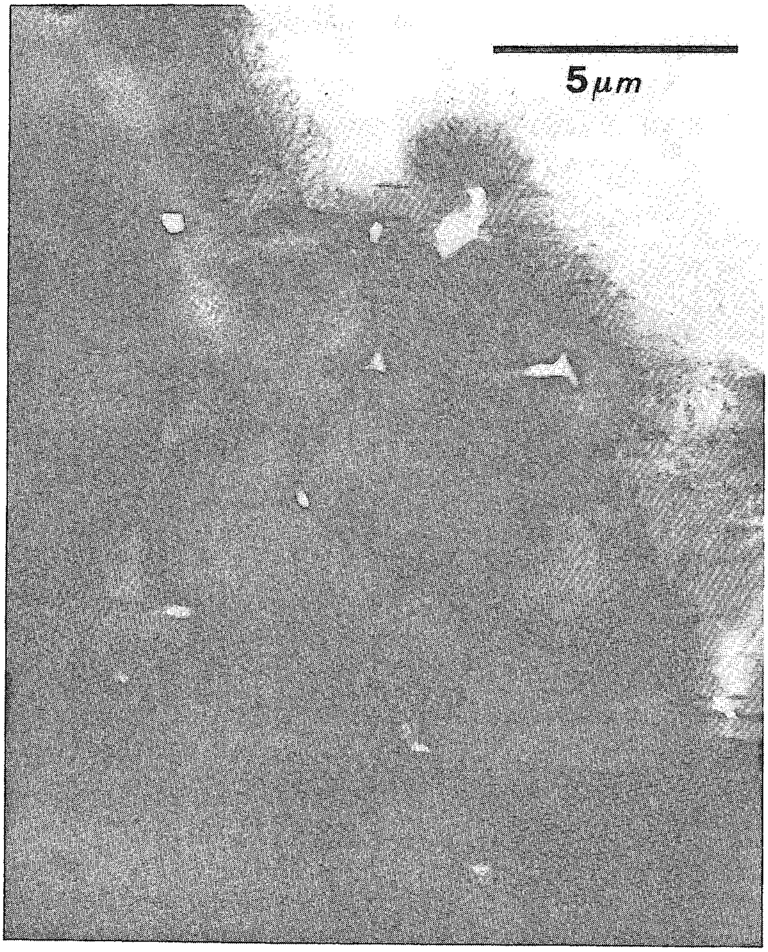

FIG. 6. A high density of twins in opaque, copper-rich sphalerite with voids at the twin intersections. The twins are developed on {111}.

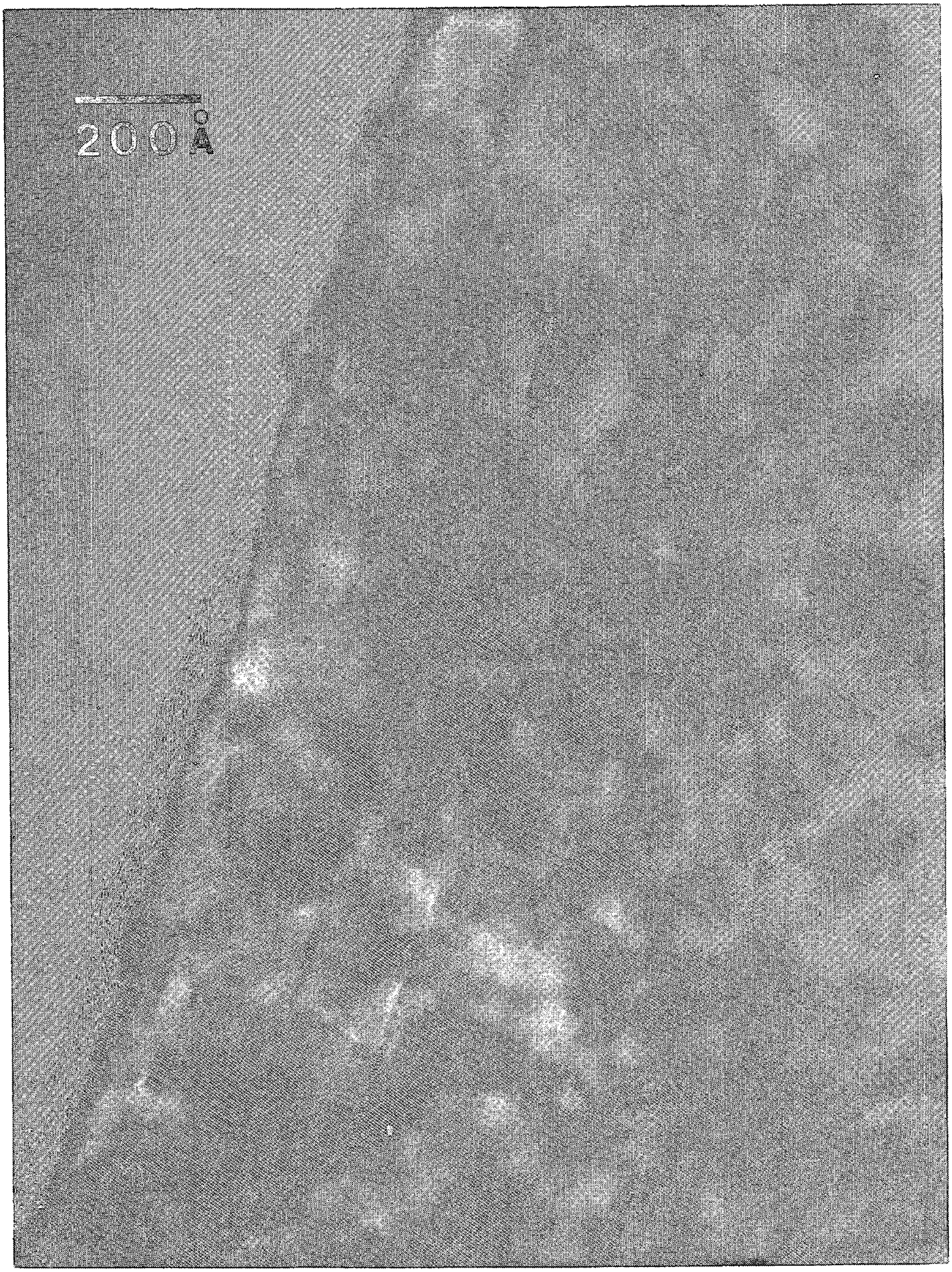

FIG. 7. Electron micrograph displaying a system of platelets on {111} in the copper-rich sphalerite that have the characteristics of GP zones.

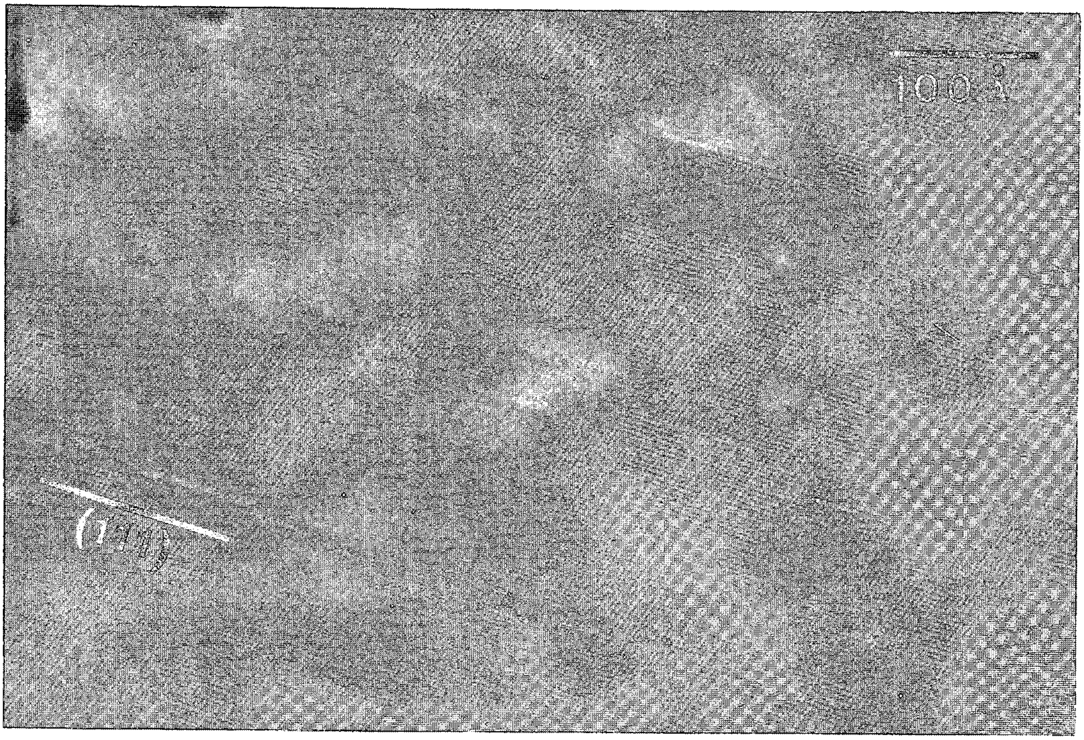

FIG. 8. Electron micrograph showing a high-resolution lattice image of the copper-rich sphalerite (detail of Fig. 7). The GP zones developed on {111} are clearly visible, as is the sphalerite lattice.

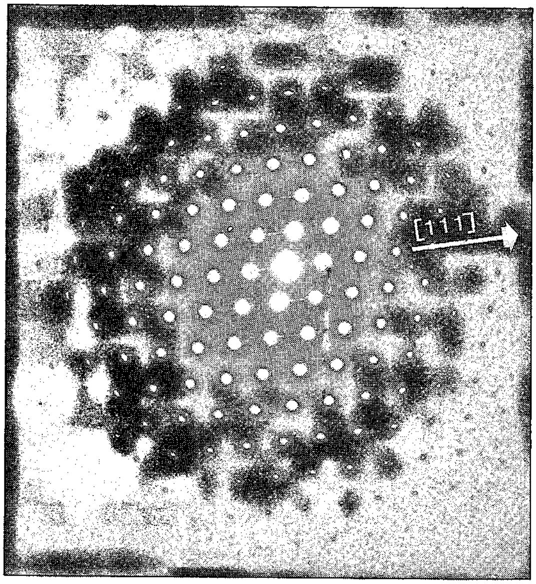

FIG. 9. Selective-area diffraction pattern of the copper-rich sphalerite (Fig. 8), the streaking corresponding to the development of GP zones on {111}.

DISCUSSION

Substitution of indium and copper for zinc

The solubility of indium in sphalerite under experimental conditions is very low: only 25 ppm at 500°C (Kissin 1972). Similar experimental studies of copper solubility in sphalerite in the system Cu–Zn–Fe–S have shown that at ambient temperatures, it is less than 0.5 wt% (Wiggins & Craig 1980). However, several wt% of both copper and indium have been detected in sphalerite using EMPA, where both elements are present in the structure (Burke & Kieft 1980). In this study, the clear correlation between copper and indium enrichment has again been demonstrated. The absence of any particles in the indium-rich zones and the undisturbed structure shows that the indium and copper are genuinely incorporated into the sphalerite. The structural similarities between roquesite and sphalerite indicate this to be a simple substitution of $Cu^+ + In^{3+} = 2Zn^{2+}$. Presumably, a similar mechanism involving copper and ferric iron (chalcopyrite and roquesite are isostructural) is inhibited by incorporation of iron in ZnS as Fe^{2+}.

Cu-rich particles

Three processes could account for the development of the chalcopyrite particles: primary precipitation, exsolution, and replacement. The distribution of the particles parallel to the growth banding suggests that they are a primary feature, related in some way to the growth of the iron-rich sub-bands. The regular distribution and ellipsoidal shape of the particles, however, have similarities to textures seen in the exsolution of chalcopyrite in natural and synthetic sphalerite, as discussed by Wiggins & Craig (1980). Solubilities of CuS in (Zn,Fe)S are low, less than 2.4 mol.% at 300°C (Kojima & Sugaki 1985) and at 25°C, as low as 0.5 wt% Cu (Wiggins & Craig 1980). Nonetheless, the particles observed in this study are volumetrically a very small component of the sphalerite (< 0.5 wt%) and could represent the amount of copper that can be dissolved in sphalerite at the temperature of mineralization, 160°C (Pattrick & Bowell 1991). On cooling, the excess copper reacted with the FeS component of the sphalerite to form chalcopyrite. This would indicate a higher initial concentration of copper in these iron-rich sub-bands than in the rest of the sphalerite.

The development of chalcopyrite blebs in sphalerite by replacement is a well-recognized phenomenon, as is the selective development of these particles in iron-rich bands (Barton & Bethke 1987, Eldridge *et al.* 1983). In the Shropshire veins, a paragenetically late generation of chalcopyrite does occur, and there is evidence of some replacement of the sphalerite in the form of crystallographically controlled rows of particles, especially in iron-rich bands. It is therefore possible that all the sphalerite has been affected by a pervasive Cu-rich fluid, which has resulted in very selective replacement of iron-rich bands (*cf.* Barton & Bethke 1987). However, the regularity of the rows of inclusions observed in this TEM investigation strongly suggests that replacement is not the mechanism of formation of the particles described here.

The opaque sphalerite

The development of the opaque sphalerite is clearly related to the reaction with later fluids; the GP zones are considered the product of this process. GP zones are usually formed by exsolution, but in this sample it appears to be the introduction of copper into the sphalerite that has caused their formation. The twinned nature of the sphalerite and the development of voids will have greatly aided the introduction of the copper, but the pervasive nature of the chalcopyrite platelets indicate that copper diffusion through the sphalerite also occurred. Thus, the GP zones may have developed by a change in composition causing the system to move into the two-phase field, rather than by a decrease in temperature.

Although there is no direct information on the exact composition of the GP zones, they may well represent the earliest development of chalcopyrite in the sphalerite. This is a very common replacement phenomenon involving the reaction of copper with the iron component of (Zn,Fe)S (Eldridge *et al.* 1983) that leads to the formation of chalcopyrite particles in the sphalerite. Diffraction analysis indicates the GP zones and the host sphalerite to have the same structure, further supporting the case for chalcopyrite.

The nature of the voids is uncertain, but they may represent the location of secondary fluid inclusions at twin intersections.

The generation of the Fe–Cd–In–Cu-rich bands

Studies of fluid inclusions (Pattrick & Bowell 1991) suggest that fluids precipitated sphalerite at temperatures ranging from 200 to 120°C (mostly around 150°C). The fluids were highly saline $CaCl_2$-dominated brines, with chloride concentrations of several molal. Although there are insufficient data to deduce fluid pH or $\log f(O_2)$, McLimans *et al.* (1980) and Giordano & Barnes (1981) have deduced pH values from neutral to 2 log units acid (5.8 to 3.8 at 150°C) and $\log f(O_2)$ of around –50 at 150°C (*i.e.*, well within the field of predominance of reduced sulfur species) for similar Pb–Zn–Ba deposits.

The compositional banding suggests that periodic changes in the chemical or physical properties of the ore-forming fluid must have taken place. The observed distribution of trace-element-enriched zones may be due to either equilibrium or kinetic effects.

The equilibrium distribution of trace elements in sphalerite is governed by the composition of the hydrothermal fluid and by the thermodynamic equilibrium constant for the exchange reaction:

$$\mathrm{ZnS\ (sp)} + M^{2+}\mathrm{(aq)} = M\mathrm{S\ (sp)} + \mathrm{Zn}^{2+}\mathrm{(aq)}$$

Thus Fe-rich sphalerite could be produced either by an increase in the ratio of total dissolved iron to dissolved zinc in solution, $\Sigma\mathrm{Fe}/\Sigma\mathrm{Zn}$, or by a change in concentration of potential metal-complexing ligands in solution. Indeed, Mookherjee (1962) proposed that temperature- and ionic-strength-dependent differences in the stabilities of Zn and Cd chloride complexes may account for the large variations that may be found in the Cd contents of sphalerite. Zinc is more effectively complexed by chloride ligands over the temperature range 100 – 150°C than is iron (Fig. 10). Thus, an increase in chloride concentration of a sphalerite-precipitating solution will lead to an increase in $(a_{\mathrm{Fe}^{2+}}/a_{\mathrm{Zn}^{2+}})/(\Sigma\mathrm{Fe}/\Sigma\mathrm{Zn})$, which in turn will result in a more Fe-rich sphalerite being precipitated [provided ($\Sigma\mathrm{Fe}/\Sigma\mathrm{Zn}$) remains constant]. Figure 11 shows how the relative free concentrations of the metal ions Fe^{2+}, Cu^{2+} Cd^{2+} and In^{3+} vary with chloride ion concentration at 150°C. An increase in concentration of the chloride ion from 1 to 4 molal will greatly increase the Fe and Cu contents of any precipi-

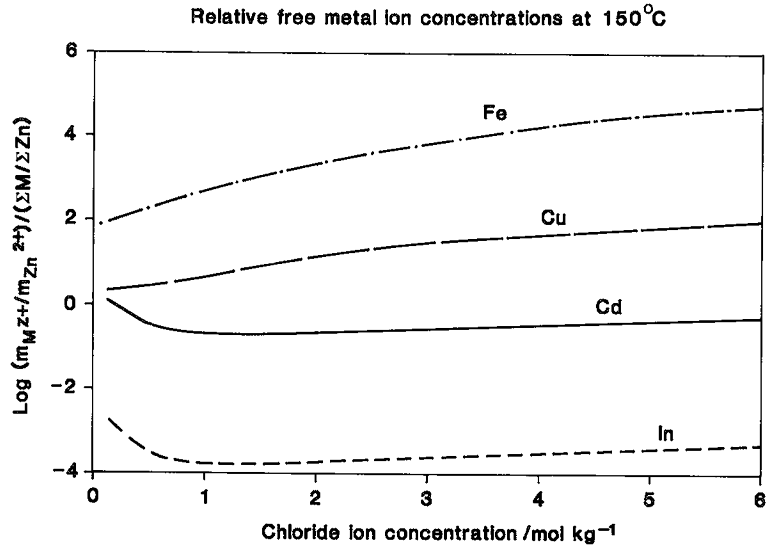

FIG. 10. Relative concentrations of the free metal ions Fe, Cu, Cd and In relative to Zn as a function of chloride ion concentration at 150°C. This parameter is expressed as log ($m_{M^{z+}}/m_{Zn^{2+}}$)/(Σ*M*/ΣZn), where Σ*M* and ΣZn refer to the total dissolved concentration of metal, *M*, and zinc respectively. The parameters at 100°C are closely similar to those presented here. Plotted from data presented in Table 2.

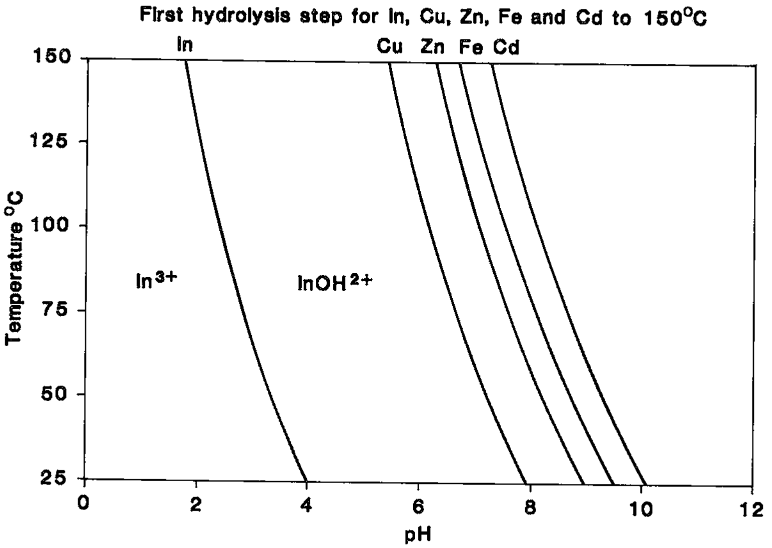

FIG. 11. The first hydrolysis constant for In, Cu, Zn, Fe and Cd at temperatures from 25° to 150°C. Plotted from data presented in Table 2. Each curve represents the boundary between the predominance fields of a given free metal ion and its monohydroxy complex.

tated sphalerite and will slightly increase the Cd and In contents. A closely similar trend is observed at 100°C. Thus, the observed pattern of trace element zoning here may be due to changes in the chlorinity of the ore-forming fluid. However, it is difficult to envisage a mechanism by which changes in chlorinity could produce the equilibrium separation of Fe+Cd- from Cu+In-rich bands.

Changes in the oxygen fugacity or sulfur fugacity of an ore-forming fluid may lead to changes in the level of trace elements in the sphalerite. Notably, Barton *et al.* (1977) invoked periodic influxes of relatively reduced fluid to produce bands of relatively iron-rich sphalerite in the OH vein, Creede, Colorado. The described relationship between Fe-content of sphalerite and log $f(O_2)$ and log $f(S_2)$ assumes saturation of the fluid with pyrite. The absence of pyrite in the sphalerite bands described in this study, however, means that the model of Barton *et al.* (1977) is not applicable.

The effect of changes in oxygen fugacity on metal-complexing has been considered here as a possible explanation for the observed trace-element zoning and has been rejected. The absence of barite suggests that the ore-forming fluids were characterized by oxygen fugacities at which reduced sulfur(II) species predominated. Under these conditions, Fe, Zn, Cd and In would not be expected to undergo any significant change in the dominant valence state of the dissolved species (Chen *et al.* 1983). Only Cu might exhibit a change from predominantly Cu(I) to Cu(II) valence states; such a change for just Cu clearly cannot explain the enrichment in Fe and Cd associated with the Cu-rich bands in sphalerite.

It is likely that variations in $a_{Fe^{2+}}/a_{Zn^{2+}}$ may be brought about by changes in the bulk composition of the fluid or by changes in the concentrations of ligands not considered here, particularly bisulfide ion and various carboxylic acids. There are insufficient data to fully assess these possibilities.

An alternative approach to explain the sphalerite banding observed in this study is to invoke disequilibrium processes. Oen *et al.* (1980) suggested nonequilibrium crystallization of a supercooled hydrothermal fluid with diffusion-controlled cyclic supersaturation at the sphalerite-fluid interface to explain oscillatory zoning in sphalerite at Cartagena, Spain. Roedder (1968) suggested secondary (postdepositional) diffusion to explain compositional banding in an analogous fashion to Liesegang rings; however, such a process would be expected to produce anhedral bands in contrast to bands along crystal faces ubiquitously observed in this study.

Incorporation of trace elements will be enhanced by rapid rates of precipitation (*cf.* Lorens 1981), in turn brought about by an increase in supersaturation of the ore-forming fluid. Such an increase in sphalerite supersaturation might be brought about by a decrease in temperature, by an increase in total dissolved reduced sulfur, or by an increase in pH. Of these changes, a pH increase may serve to separate Fe+Cd and Cu+In because of the pH dependence of their adsorption onto sphalerite surfaces.

Inorganic sorption is highly effective in controlling the metal ion content of river and groundwaters (Hem 1972). The extent of sorption is strongly pH-dependent, typically occurring over a narrow range of pH. James & MacNaughton (1977) found that heavy metals are adsorbed onto inorganic minerals over a pH range corresponding to the transition between the predominance of nonhydrolyzed and hydrolyzed metal species. That is, sorption is strongly favored by the formation of metal hydroxide species:

$$Fe^{2+}\,(aq) + OH^-\,(aq) = Fe(OH)^+\,(aq)$$

Furthermore, Jean & Bancroft (1986) reported enhanced Cd adsorption onto sphalerite when the pH is increased to a value 2 or 3 log units below the first hydrolysis constant of Cd. Since In, Cu, Fe and Cd have different values of the first hydrolysis constant, this mechanism may provide a means of separating these elements in the sphalerite bands observed in this study.

The first hydrolysis constants for In, Cu, Fe and Cd over the temperature range 25°C to 150°C are shown in Figure 11. Indium is clearly largely hydrolyzed over the entire range of pH conditions expected for the sphalerite bands, whereas an increase in pH from 3 1/2 to 5 1/2 at 150°C would be expected to successively lead to the adsorption of Cu, then Fe, then Cd. This sequence of maximum adsorption closely matches the observed compositional banding. Particularly where the effective radius and charge distribution of the adsorbed ion are similar to those of Zn^{2+}, the adsorption process is likely

TABLE 2. THERMODYNAMIC STABILITY OF SELECTED CHLORO AND HYDROXY COMPLEXES OF INDIUM, CADMIUM, COPPER, IRON AND ZINC FROM 25°C TO 150°C

Equilibrium	log (Equilibrium constant) 25°C	60°C	100°C	150°C	Ref
$In^{3+} + Cl^- = InCl^{2+}$	2.43	2.61	2.81	3.19	a
$In^{3+} + 2Cl^- = InCl_2^+$	3.43	3.75	4.15	4.92	a
$In^{3+} + 3Cl^- = InCl_3^0$	3.63	4.65	5.68	7.24	a
$Cd^{2+} + Cl^- = CdCl^+$	1.37	1.47	1.63	1.98	b
$Cd^{2+} + 2Cl^- = CdCl_2^0$	2.21	2.25	2.47	3.07	b
$Cd^{2+} + 3Cl^- = CdCl_3^-$	2.40	2.83	3.34	4.09	b
$Cu^{2+} + Cl^- = CuCl^+$	0.01	0.72	1.54	2.57	c
$Cu^{2+} + 2Cl^- = CuCl_2^0$	−0.69	0.16	1.15	2.36	c
$Cu^{2+} + 3Cl^- = CuCl_3^-$	−2.29	−1.23	0.04	1.52	c
$Fe^{2+} + Cl^- = FeCl^+$	−0.16		0.21	0.66	d
$Zn^{2+} + Cl^- = CdCl^+$	0.42		1.83	2.86	e
$Zn^{2+} + 2Cl^- = CdCl_2^0$	0.62		1.89	2.90	e
$Zn^{2+} + 3Cl^- = CdCl_3^-$	0.34		1.30	2.10	e
$Zn^{2+} + 4Cl^- = ZnCl_4^{2-}$	0.19		2.10	3.06	e
$H^+ + Cl^- = HCl^0$	−0.71		−0.64	−0.49	f
$In^{3+} + H_2O = InOH^{2+} + H^+$	−4.00	−3.12	−2.42	−1.75	g
$Cd^{2+} + H_2O = CdOH^+ + H^+$	−10.08	−9.05	−8.13	−7.22	g
$Cu^{2+} + H_2O = CuOH^+ + H^+$	−7.93	−7.00	−6.19	−5.39	g
$Fe^{2+} + H_2O = FeOH^+ + H^+$	−9.50	−8.48	−7.56	−6.65	g
$Zn^{2+} + H_2O = ZnOH^+ + H^+$	−8.96	−7.97	−7.09	−6.24	g

Where unavailable, data for metal-complex stabilities have been extrapolated from published 25°C data using the estimation technique of Criss & Cobble (1964) for average ionic heat capacities:

$$C_{p,i}]^{T}_{Tr} = \alpha(T) + \beta(T)\{ S_i(Tr) + Z_i S_{H^+}^{(abs)}(Tr) \}$$

where $C_{p,i}]^{T}_{Tr}$ is the heat capacity, C_P, of ion, i, over the temperature range T_r to T, and where α and β are temperature dependent constants for a particular ion-type (e.g. cations, oxygen free anions) tabulated by Criss & Cobble (1964), $S^{H_+}{}^{(abs)}(Tr)$ is the absolute molar entropy of $H^+(aq)$ at the reference temperature, Tr, Z_i is the ionic charge of the species, i, and $S_i(Tr)$ is the molar entropy of thre species, i, at the refrence temperature. The reference temperature was taken to be 298.15 K. A value of −5.0 cal/K/mol was adopted for $S_{H^+}^{(abs)}(Tr)$ after Criss and Cobble (1964).

The veracity of the method was checked by comparing calculated and experimental stability constants for zinc-chloride and iron-chloride complex formation. Agreement between calculated and experimental values [Zn: Ruaya & Seward (1987); Fe: Heinrich & Seward (1990)] is better than ½ a log unit except for $ZnCl_4^{2-}$, for which the method works poorly because of a change of complex symmetry from $ZnCl_3^-$ to $ZnCl_4^{2-}$ (Ruaya 1988).

Sources of data: a Extrapolated in this study from 25°C data of Tuck (1983). b Extrapolated in this study from 25°C data of Garrels & Christ (1965). c Wolery (1988). d Heinrich and Seward (1990). e Ruaya and Seward (1986) - smoothed data. f Ruaya & Seward (1986). g Extrapolated in this study from 25°C data of Baes & Mesmer (1981), Weast (1976) and Garrels & Christ (1965).

to be very strong and may become irreversible (Hem 1972), leading ultimately to the incorporation of the adsorbed ion into the crystal structure of sphalerite. Thus the adsorption of Fe^{2+} and Cu^{2+}, which have ionic radii very similar to that of Zn^{2+} in 4-coordinated sites, is likely to be much stronger and more irreversible than that for In^{3+} and Cd^{2+}, which are significantly larger ions (Shannon 1981). It further seems likely, therefore, that the incorporation of the relatively poorly adsorbed indium may depend critically upon the adsorption of Cu^{2+} and the dissolution of particles of the isostructural roquesite on and within the sphalerite.

The events that caused the periodic changes in pH of the fluid leading to formation of the sphalerite banding may be related to (i) changes in source fluid or (ii) changes in degree of mixing of hydrothermal fluid with surface or near-surface waters. Periodic inputs of magmatic waters have been suggested by Barton *et al.* (1977) as a cause of sphalerite banding at Creede, Colorado. The absence of nearby coeval igneous bodies in West Shropshire leads us to eliminate this as a possible model in this case. Considered more likely are periodic inputs of hydrothermal fluid due to cyclic reactivation of faults (with transient permeabilities) (*cf.* Sibson 1981, Sibson *et al.* 1988): this would result in the sudden influx of relatively rapidly moving high-temperature fluids poorly equilibrated with the country rock, followed by a gradual decrease in flow rate, temperature and hydrogen ion activity. Such cycling would be expected to produce a sharp boundary between new Fe-poor sphalerite and older Fe-rich sphalerite, and a somewhat diffuse boundary between new Fe-rich sphalerite and older Fe-poor sphalerite; this set of boundaries was not observed in the West Shropshire veins.

Seasonal variations in groundwater levels, leading to varying degrees of mixing, have been proposed by Roedder (1968) to explain basin-wide banding in sphalerite. Horbury & Adams (1989) explained banded carbonate cements in the late Dinantian of the English Lake District as being due to varying degrees of fluid mixing as a result of cyclic changes in sea level. However, McLimans *et al.* (1980) dismissed groundwater mixing as an explanation for basin-wide banding in sphalerite on the basis that such a process would produce more irregular textures, without consistently sharp boundaries between compositionally distinct bands.

In summary, we favor the formation of banding in sphalerite as a result of disequilibrium crystallization in response to cyclic changes in pH and possibly, less importantly, temperature. The variation in the first hydrolysis step of the various trace elements incorporated is the key to the chemical separation of In+Cu from Fe+Cd in sphalerite, due to preferential adsorption of these elements over different ranges of pH. There is insufficient evidence at present to determine fully the geological processes resulting in such cyclic chemical changes, but it appears likely that they are related either to cyclic pumping (*cf.* Sibson 1981) of source fluid or to periodic changes in the extent of mixing of the hydrothermal fluid with groundwaters.

ACKNOWLEDGEMENTS

The authors are grateful to Ian Brough, Graham Cliff and Peter Kenway for invaluable assistance with the TEM analysis, and to Professor G.W. Lorimer and Dr. P.E. Champness for useful discussions. The final manuscript also benefitted greatly from the comments of three unnamed referees. Financial support was provided by NERC grant GR3/7197.

REFERENCES

ANDERSON, J.S. (1953): Observations on the geochemistry of indium. *Geochim. Cosmochim. Acta* **4**, 225-240.

BAES, C.F., JR. & MESMER, R.E. (1981): The thermodynamics of cation hydrolysis. *Am. J. Sci.* **281**, 935-962.

BARTON, P.B., JR. & BETHKE, P.M. (1987): Chalcopyrite disease in sphalerite: pathology and epidemiology. *Am. Mineral.* **72**, 451-467.

——, —— & ROEDDER, E. (1977): Environments of ore deposition in the Creede mining district, San Juan Mountains, Colorado. III. Progress towards interpretation of the chemistry of the ore-forming fluid for the OH vein. *Econ. Geol.* **72**, 1-24.

BURKE, E.A.J. & KIEFT, C. (1980): Roquesite and Cu–In-bearing sphalerite from Långban, Bergslagen, Sweden. *Can. Mineral.* **18**, 361-363.

CHAMPNESS, P.E. & LORIMER, G.W. (1976): Exsolution in silicates. *In* Electron Microscopy in Mineralogy (H.-R. Wenk, ed.). Springer-Verlag, Berlin (174-204).

CHEN, C.M., ARAL, K. & THEUS, G.J. (1983): Computer-calculated potential pH diagrams to 300°C. 2. Handbook of diagrams. *Nat. Tech. Inf. Serv., EPRI* **NP-3137**.

CLIFF, G. & LORIMER, G.W. (1975): The quantitative analysis of thin specimens. *J. Microsc.* **103**, 203-207.

CRISS, C.M. & COBBLE, J.W. (1964): The thermodynamic properties of high temperature aqueous solutions. IV. Entropies of the ions up to 200°C and the correspondence principle. *J. Am. Chem. Soc.* **86**, 5385-5390.

ELDRIDGE, C.S., BARTON, P.B., JR. & OHMOTO, H. (1983): Mineral textures and their bearing on the formation of the Kuroko orebodies. *Econ. Geol., Monogr.* **5**, 241-281.

GARRELS, R.M. & CHRIST, C.L. (1965): *Solutions, Minerals and Equilibria.* Freeman, Cooper and Co., San Fransisco, California.

GIORDANO, T.H. & BARNES, H.L. (1981): Lead transport in

Mississippi Valley-type ore solutions. *Econ. Geol.* **76**, 2200-2211.

HAK, J., KVAČEK, M. & WATKINSON, D.H. (1983): Indium content of sphalerite from Turkank zone in the Kutna base metal deposit (Bohemia). *Cas. Mineral. Geol.* **28**, 65-69.

HEINRICH, C.A. & SEWARD, T.M. (1990): A spectrophotometric study of aqueous iron(II) chloride complexing from 25 to 200°C. *Geochim. Cosmochim. Acta* **54**, 2207-2221.

HEM, J.D. (1972): Chemistry and occurrence of cadmium and zinc in surface water and groundwater. *Water Resources Res.* **8**, 661-679.

HORBURY, A.D. & ADAMS, A.E. (1989): Meteoric phreatic diagenesis in cyclic late Dinantian carbonates, northwest England. *In* Zoned Carbonate Cements: Techniques, Applications and Implications (B.W. Sellwood, ed.). *Sed. Geol.* **65**, 319-344.

JAMES, R.O. & MACNAUGHTON, M.G. (1977): The adsoprtion of aqueous heavy metals on inorganic minerals. *Geochim. Cosmochim. Acta* **41**, 1549-1555.

JEAN, G.E. & BANCROFT, G.M. (1986): Heavy metal adsorption by sulphide mineral surfaces. *Geochim. Cosmochim. Acta* **50**, 1455-1463.

JOHAN, Z. (1988): Indium and germanium in the structure of sphalerite: an example of coupled substitution with copper. *Mineral. Petrol.* **39**, 211-229.

KISSIN, S.A. (1972): An investigation of the solubility of indium in hydrothermally synthesized galena and sphalerite. *Can. Mineral.* **11**, 575. (abstr.).

KOJIMA, S. & SUGAKI, A. (1985): Phase relations in the Cu–Zn–Fe–S system between 500 and 300°C under hydrothermal conditions. *Econ. Geol.* **80**, 158-171.

LORENS, R.B. (1981): Sr, Cd, Mn and Co distribution coefficients in calcite as a function of calcite precipitation rate. *Geochim. Cosmochim. Acta* **45**, 553-561.

MCLIMANS, R.K., BARNES, H.L. & OHMOTO, H. (1980): Sphalerite stratigraphy of the Upper Mississippi Valley lead–zinc district, southwest Wisconsin. *Econ. Geol.* **75**, 351-361.

MOOKHERJEE, A. (1962): Certain aspects of the geochemistry of cadmium. *Geochim. Cosmochim. Acta* **26**, 351-360.

NORD, G.L., JR. (1980): The composition, structure and stability of Guinier–Preston zones in lunar and terrestial orthopyroxene. *Phys. Chem. Minerals* **6**, 109-128.

OEN, I.S., KAGER, P. & KIEFT, C. (1980): Oscillatory zoning of a discontinuous solid-solution series: sphalerite–stannite. *Am. Mineral.* **65**, 1220-1232.

PATTRICK, R.A.D. & BOWELL, R.J. (1991): The genesis of the West Shropshire Orefield: evidence from fluid inclusions, sphalerite chemistry, and sulphur isotopic ratios. *Geol. J.* **26**, 101-115.

ROEDDER, E. (1968): The noncolloidal origin of "colloform" textures in sphalerite ores. *Econ. Geol.* **63**, 451-471.

RUAYA, J.R. (1988): Estimation of instability constants of metal chloride complexes in hydrothermal solutions up to 300°C. *Geochim. Cosmochim. Acta* **52**, 1983-1966.

_____ & SEWARD, T.M. (1986): The stability of chlorozinc(II) complexes in hydrothermal solutions up to 350°C. *Geochim. Cosmochim. Acta* **50**, 651-661.

_____ & _____ (1987) The ion-pair constant and other thermodynamic properties of HCl up to 350°C. *Geochim. Cosmochim. Acta* **51**, 121-130.

SHANNON, R.D. (1981): Bond distances in sulfides and a preliminary table of sulfide crystal radii. *In* Structure and Bonding in Crystals **II** (M. O'Keeffe & A. Navrotsky, eds.). Academic Press, New York (53-70).

SIBSON, R.H. (1981): Fluid flow accompaning faulting: field evidence and models. *In* Earthquake Prediction: an International Review. (D.H. Simpson, D.H. & P.G. Richard, eds.). *Am. Geophys. Union, Maurice Ewing Ser.* **4**, 593-603.

_____, ROBERT, F. & POULSON, K.H. (1988): High-angle reverse faults, fluid-pressure cycling and mesothermal gold–quartz deposits. *Geology* **16**, 551-555.

TIGHE, N.J. (1976): Experimental techniques. *In* Electron Microscopy in Mineralogy (H.-R. Wenk, ed.). Springer-Verlag, Berlin (144-171).

TUCK, D.G. (1983): Critical survey of stability constants of complexes of indium. *Pure Appl. Chem.* **55**, 1477-1528.

WEAST, R.C. (1976): *CRC Handbook of Chemistry and Physics* (56th ed.). CRC Press, Cleveland, Ohio.

WIGGINS, L.B. & CRAIG, J.R. (1980): Reconnaissance of the Cu–Fe–Zn–S system: sphalerite phase relationships. *Econ. Geol.* **75**, 742-751.

WOLERY, T. (1988): EQ3 computer code. *Lawrence Livermore National Laboratory, File* **DATA0.3245R54** (last update 18 Feb. 1988).

Received October 15, 1991, revised manuscript accepted June 30, 1992.